Microchimica Acta (2019) 186: 250
https://doi.org/10.1007/s00604-019-3360-6

ORIGINAL PAPER

Colorimetric determination of lead(II) or mercury(II) based on target induced switching of the enzyme-like activity of metallothionein-stabilized copper nanoclusters

Ran Liu[1] · Li Zuo[1] · Xiaorong Huang[1] · Shimeng Liu[1] · Guiying Yang[1] · Shiya Li[1] · Changyin Lv[1]

Received: 24 November 2018 / Accepted: 8 March 2019 / Published online: 19 March 2019

Abstract

It is shown that metallothionein-stabilized copper nanoclusters (MT-CuNCs) display catalase-like activity. In the presence of either lead(II) or mercury(II), the catalase-like activity is converted to a peroxidase-like activity. On addition of Pb(II) or Hg(II), the inhibitory effect of MT-CuNCs on the chromogenic reaction of 3,3′,5,5′-tetramethylbenzidine (TMB) with H_2O_2 is weakened. On the other hand, the catalytic effect of the nanoclusters on the chromogenic reaction is increased. The system MT-CuNCs-Pb(II)/Hg(II) exhibits high affinity for the substrates TMB and H_2O_2. Their catalytic behavior follows Michaelis-Menten kinetics. Based on these findings, a method was developed for visual detection (via the blue coloration formed) and spectrophotometric determination (at 450 nm) of Pb(II) and Hg(II). The linear range for Pb(II) extends from 0.7 to 96 μM, and the linear ranges for Hg(II) from 97 nM to 2.3 μM and from 3.1 μM to 15.6 μM. The detection limits are 142 nM for Pb(II) and 43.8 nM for Hg(II).

Keywords Nanozymes · Catalase-like activity · Peroxidase-like activity · Pb-Cu/Hg-Cu alloy · Heavy metal · Environmental samples

Introduction

Catalase is an antioxidant enzyme that catalyzes the decomposition of H_2O_2 into O_2 and H_2O. Catalase can effectively scavenge H_2O_2 in vivo so that H_2O_2 cannot react with O_2 under the action of iron chelates to produce highly oxidative hydroxyl radicals (·OH) [1]. Natural peroxidase is an enzyme that catalyzes the oxidation of specific substrates by providing electrons for H_2O_2 (electron acceptor). Natural enzymes catalyze reactions under very mild biological conditions, which limits their applications [2]. Compared to natural enzymes, many artificial nanozymes, such as carbon nanotubes, magnetic nanomaterials [3, 4], noble metal-graphene complexes [5], and metal nanoclusters [6, 7], have the advantages of simple manufacturing, low cost, high catalytic activity, good stability, etc. [8]. In particular, metal nanoclusters have been widely applied [9].

Lead and mercury ions can pollute the environment and endanger health. In order to quantify the concentration of Pb(II) and Hg(II) in water samples, analytical methods such as inductively coupled plasma mass spectrometry (ICP-MS), atomic absorption spectroscopy (AAS) and electrochemical analysis have been developed. The disadvansatages of these methods are bulky instruments, high cost, the need for professionally operators [10, 11]. Therefore, it is still highly desirable to develop a rapid and convenient method for detecting Pb(II) and Hg(II).

Pb(II) and Hg(II) can inhibit or enhance the activity of artificial nanozymes under certain conditions thus establishing a new method for detecting Pb(II) or Hg(II). Zhu [12] et al. found that Hg^{2+} inhibited the peroxidase-like activity of bovine serum albumin-capped AuNCs via Au^{+}-Hg^{2+} interaction. Liao [13] et al. developed a Pb^{2+} assay due to the ability of Pb^{2+} to induce the aggregation of glutathione (GSH) stablized AuNCs and enhance their peroxidase-like activity. Tseng [14]

Electronic supplementary material The online version of this article (https://doi.org/10.1007/s00604-019-3360-6) contains supplementary material, which is available to authorized users.

✉ Changyin Lv
lchy1955@163.com

[1] College of Public Health, University of South China, Hengyang 421001, People's Republic of China

et al. prepared bimetallic Pt/Au NPs and found that Hg^{2+} transformed this peroxidase-like activity into a catalase-like activity. Yuan [15] et al. researched that the peroxidase-like activity of molybdenum disulfide nanosheets (MoS_2-NSs) was stimulated by Hg^{2+}. Most of the platforms in related reports are based on the use of the Hg^{2+}-Au^{+} reaction to change the enzyme activity of gold-containing nanozymes. By contrast, a study on the modfication of copper nanoclusters with enzyme-mimicking activity based on the heavy metal ions Pb^{2+} and Hg^{2+} has not been reported.

Herein, the effects of the heavy metal ions Pb^{2+} and Hg^{2+} on the enzyme-like activity of MT-CuNCs were explored, and Pb^{2+} and Hg^{2+} assay strategies were established. It is found that MT-CuNCs have catalase-like activity and that Pb^{2+}/Hg^{2+} can induce the conversion of this catalase-like activity to peroxidase-like activity. Under certain conditions, H_2O_2 can self-oxidize to produce a small number of hydroxyl radicals (·OH), thus oxidizing TMB to 3,3′,5,5′-tetramethylbenzidine diimine (oxTMB). Correspondingly, the solution changes from colorless to light blue (Scheme 1a). The MT-CuNCs have catalase-like activity, which can decompose H_2O_2 and inhibit the oxidation of TMB. The solution color consequently become lighter (Scheme 1b). In the presence of Pb^{2+} or Hg^{2+}, the catalase-like activity of the MT-CuNCs can be converted into peroxidase-like activity, thus catalyzing the oxidation and chromogenic reaction of TMB mediated by H_2O_2. Therefore, the solution changes from colorless to dark blue (Scheme 1c). Accordingly, a detection of Pb^{2+} or Hg^{2+} based on colorimetry and spectrophotometry was established. This detection method is selective,and feasible and has a wide linear range. The development of this method is informative for the progress of enzyme mimics.

Experimental section

Reagents and materials Pb^{2+} and Hg^{2+} standard solutions were supplied by the Chinese Academy of Metrology (Beijing, China, www.nim.ac.cn). MT (induced by Zn^{2+} with a purity higher than 99%) was acquired from Yongkang Jiaxin Biological Technology Co., Ltd. (Beijing, China, www.jiaxintool.cn.globalimporter.net). $CuCl_2$, catalase (CAT), TMB, phosphate buffered saline (PBS), 2′-diamino-bis-3-ethylbenzothiazolin-6-sulfonic acid (ABTS) and absolute ethanol were supplied by McLean Biochemical Technology Co., Ltd. (Shanghai, China, www.macklin.company.com). NaOAc, H_2O_2 and H_2SO_4 were obtained from Beijing Chemicals Reagent Company (Beijing, China, www.bicr.com). The electrical resistivity of the ultrapure water used was 18.25 MΩ·cm.

Apparatus All ultraviolet-visible absorbance spectra obtained using a Shimadzu UV-2450 spectrophotometer (Kyoto, Japan, www.shimadzu.com). A THERMO-SHAKER thermostat mixer (Heros, China) was utilized for the synthesis of the MT-CuNCs. The fluorescence spectra were acquired on a Lumina spectrofluorometer (Thermo Fisher Scientific, USA, www.thermofisher.com). A Titan G2 60–300 transmission electron microscope (FEI, USA, www.fei.com), a K-Alpha 1063 X-ray photoelectron spectrometer (Thermo Fisher Scientific, USA, www.thermofisher.com) and a Shimadzu IR Prestige-21 Fourier transform infrared spectrometer (Kyoto, Japan, www.shimadzu.com) were used to characterize the MT-CuNCs mixed with Pb^{2+} or Hg^{2+}.

Preparation of MT-CuNCs Briefly, MT solution (600 μL, 2.25 mg·mL^{-1}) and $CuCl_2$ solution (100 μL, 3 mM) were mixed at 55 °C. NaOH solution (200 μL, 1.0 M) was added 15 min later. The reaction was proceeded with shaking at 800 rpm for 12 h at 55 °C. After filtering through a 0.22 μm filter membrane, the light purple solution was stored at 4 °C.

Determination of Pb^{2+} and Hg^{2+} In a 2 mL EP tube, NaOAc-HOAc buffer (pH 4.0, 80 μL, 200 mM), MT-CuNCs solution (30 μL), TMB solution (40 μL, 5 mM), H_2O_2 solution (60 μL, 10 mM), and a certain amount of Pb^{2+} standard solution were mixed. The reaction took place for 40 min at 40 °C in a thermostatic mixer. Then, H_2SO_4 solution (100 μL, 0.2 M) was introduced, and the measurement was performed by colorimetry. Moreover, the absorbance value of this system at 450 nm was measured.

Likewise, in a 2 mL EP tube, NaOAc-HOAc buffer (pH 3.25, 60 μL, 200 mM), MT-CuNCs solution (20 μL), TMB solution (50 μL, 5 mM), H_2O_2 solution (60 μL, 10 mM), and a certain

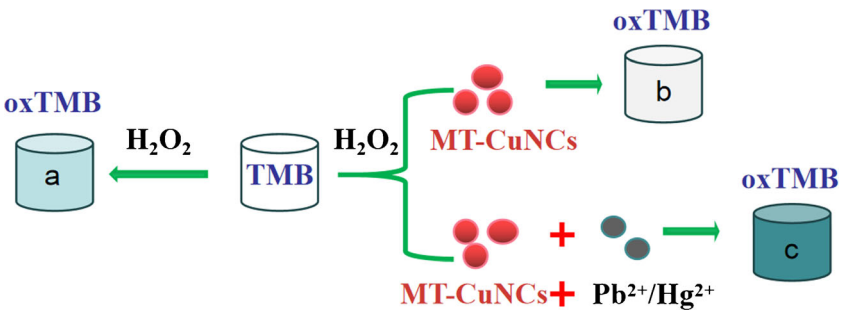

Scheme 1 Schematic presentation of the colorimetric assay for Pb^{2+}/Hg^{2+} based on target induced switching of enzyme-like activity of MT-CuNCs

amount of Hg^{2+} standard solution were mixed. The reaction took place for 40 min at 40 °C in a thermostatic mixer. Then, H_2SO_4 solution (100 μL, 0.2 M) was introduced, and the absorbance of the system at 450 nm was measured.

The absorbance change of the system was calculated as follows: $\Delta A = A - A_0$. A and A_0 represent the absorbance values in the presence and absence of Pb^{2+}/Hg^{2+}, respectively.

Results and discussion

Transformation of the enzymatic activity of MT-CuNCs induced by Pb^{2+} or Hg^{2+} The catalase-like activity of MT-CuNCs was verified by monitoring the absorbance of H_2O_2 at 240 nm, because catalase can catalyze the decomposition of H_2O_2 [16]. As shown in Fig. S1, the MT-CuNCs have high catalase-like activity and that their relative activity is 2.8 times that of the positive control group (1.5 mg·mL^{-1} CAT).

The enzyme activity transition of MT-CuNCs after the addition of Pb^{2+}/Hg^{2+} was verified by UV-Vis spectroscopy (Fig. 1a). Both TMB (a curve) and the MT-CuNCs-TMB system (b curve) have no absorption peak at 450 nm. The A_{450} of the TMB solution (c curve) increases significantly after reacting with H_2O_2, indicating that H_2O_2 may yield ·OH through self-oxidation under these conditions. The ·OH species oxidizes TMB into oxTMB. After the reaction was terminated with H_2SO_4, the solution appeared light yellow and exhibited an absorption peak at 450 nm. In the MT-CuNCs system (d curve), the TMB-H_2O_2 chromogenic reaction is suppressed, and the A_{450} value decreases. This effect may occur because MT-CuNCs with catalase-like activity catalyze the decomposition of H_2O_2 and inhibit the production of ·OH. When Pb^{2+} or Hg^{2+} was added, the A_{450} values of the MT-CuNCs-Pb^{2+}/Hg^{2+}-TMB-H_2O_2 system increased gradually with increasing Pb^{2+} or Hg^{2+} concentration, suggesting that Pb^{2+} or Hg^{2+} can convert the catalase-like activity of MT-CuNCs into peroxidase-like activity. At this time, H_2O_2 may be adsorbed on the surface of the MT-CuNCs and turned into highly active ·OH via O-O bond cleavage, thus generating the catalytic activity of the nanoclusters [17]. The kinetics of each system within 60 min were further investigated (Fig. 1b). The absorbance of the TMB-H_2O_2 system (a curve) at 652 nm increases over time. After the addition of MT-CuNCs (b curve), the absorbance value from 0 to 1700 s increases very slowly, and the slope of the kinetic curve after 1700 s is still lower than that of the TMB-H_2O_2 system. These results indicate that MT-CuNCs show catalase-like activity, which inhibites the chromogenic reaction of TMB. In the presence of Pb^{2+}/Hg^{2+} and MT-CuNCs (c, d curve), the A_{652} value increases slowly from 0 to 1200 s. Later, the slope of the kinetic curve is larger than that of the TMB-H_2O_2 system. These results confirm our hypothesis that Pb^{2+} or Hg^{2+} can reduce and transform the catalase-like activity of MTs-CuNCs into peroxidase-like activity, The latter catalyzes the oxidation reaction of TMB.

Mechanistic studies Because surface chemistry is significant in regulating electron transfer and substrate adsorption, it affects the catalytic activity of nanozymes. Liu et al. found that fluoride capping enhanced the oxidase activity of cerium oxide NPs by more than 100 times [18], while DNA increased the peroxidase activity of Fe_3O_4 NPs [19]. The mechanism of these effects was F^- and DNA regulating the surface charges of nanozymes, thereby enhancing the electron transfer and substrate adsorption on the surface of the nanozymes. In this study, the positive charges on the surface of the MT-CuNCs increased after their interaction with Pb^{2+} or Hg^{2+}, which might cause charge repulsion with positively charged TMB and weaken the catalytic activity of the MT-CuNCs in the oxidation of TMB. However, this hypothesis is not consistent with the enhancement of peroxidase activity in the experimental phenomenon. Hence, negatively charged ABTS was used

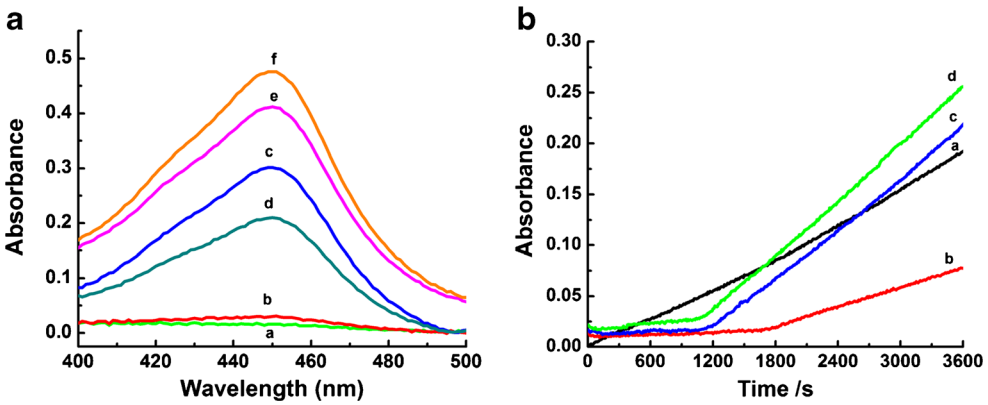

Fig. 1 Switching effects of Pb^{2+}/Hg^{2+} on enzyme-like activity of MT-CuNCs **a** Absorption spectrum of the systems with acid termination. (**a**) TMB. (**b**) TMB-MT-CuNCs. (**c**) TMB-H_2O_2. (**d**) TMB-H_2O_2-MT-CuNCs. (**e**) TMB-H_2O_2-MT-CuNCs-Hg^{2+}. (**f**) TMB-H_2O_2-MT-CuNCs-Pb^{2+}. **b** Absorbance-time curves (at 652 nm) of the systems. (**a**) TMB-H_2O_2. (**b**) TMB-H_2O_2-MT-CuNCs. (**c**) TMB-H_2O_2-MT-CuNCs-Pb^{2+}. (**d**) TMB-H_2O_2-MT-CuNCs-Hg^{2+}

as the chromatic substrate for validation (Fig. S2). The results are similar to that obtained when TMB is used as a substrate. Therefore, the transformation function of Pb^{2+}/Hg^{2+} in the enzymatic activity of MT-CuNCs should not be attributed to the regulation of surface charges.

Changes in the morphology and size of nanomaterials may affect their intrinsic properties. Liao [13] et al. found that Pb^{2+} increased the peroxidase-like activity of GSH-AuNCs and confirmed that the reason was aggregation-induced enzyme activity enhancement, similar to that of aggregation-induced luminescence. TEM images (Fig. S3) show that both Pb^{2+} and Hg^{2+} can induce the aggregation of MT-CuNCs and an increase in the size of the MT-CuNCs. With the addition of Pb^{2+} or Hg^{2+}, the photoluminescence property of the MT-CuNCs is decreased, and aggregation-induced luminescence enhancement is not observed. For further verification, the effect of Ag^{+} on the size and enzyme activity of MT-CuNCs was investigated. The size of MT-CuNCs is increased, but the absorption of oxTMB at 450 nm hardly enhance (Fig. S4). These results reveal that the enzymatic activity transformation of MT-CuNCs is not caused by the change of the morphology and size.

The catalytic activity of metal NCs and metal NPs is correlated with the valences of metal ions/complexes formed on their surfaces. Lien [20] investigated the influences of various metal ions on the oxidase activity, peroxidase-like activity and catalase-like activity, of AuNPs. They found that the formation of a metal-Au alloy over AuNPs greatly affected their catalytic performance. Therefore, in this study, the modulating function of Pb^{2+} or Hg^{2+} on the enzymatic activity of MT-CuNCs may be ascribed to the generation of Pb-Cu/Hg-Cu alloys, which was further verified by XPS (Fig. 2). The Cu 2p spectrum of MT-CuNCs show the characteristic peaks at 932.79 and 952.54 eV without the satellite peak of Cu(II) at approximately 942 eV, indicating the existence of Cu(0) and Cu(I) rather than Cu(II) (a) [21, 22]. After the interaction between MT-CuNCs and Pb^{2+}, the Cu 2p spectrum did not change significantly. The characteristic Pb 4f peaks of Pb(II) and Pb(0) are observed at 138.34/143.29 eV and 136.29/141.35 eV, respectively (b) [23]. In a pH range of 3.5–4.5, the thiolate ligands (Zn^{2+}-MT bonds) in MT were partially dissociated [24],and Pb^{2+} diffused into the α domains of MT and was reduced into Pb(0), which would be deposited on the surface of the MT-CuNCs to form a Pb-Cu alloy. In the Cu 2p spectrum of the MT-CuNCs-Hg^{2+} system (c), the characteristic satellite peak of Cu(II) is observed at 942.46 eV. Hg^{2+} might react with the Cu^{+} on the surface of the MT-CuNCs to generate Hg(0). The characteristic Hg4f peaks of Hg(II) and Hg(0) is observed at 100.86/104.91 eV and 99.54/103.59 eV, respectively (d) [25]. Hg^{2+} competed with Zn^{2+} to bind the sites in the α domains of MT, and a portion of Hg^{2+} was reduced to Hg(0) by MT. Consequently, the Pb-Cu/Hg-Cu alloy formed on the surface of the MT-CuNCs transformed their catalase-like activity into peroxidase-like activity.

The structural changes in MT-CuNCs after the addition of Pb^{2+}/Hg^{2+} (Fig. 3) were analyzed with FTIR. After the

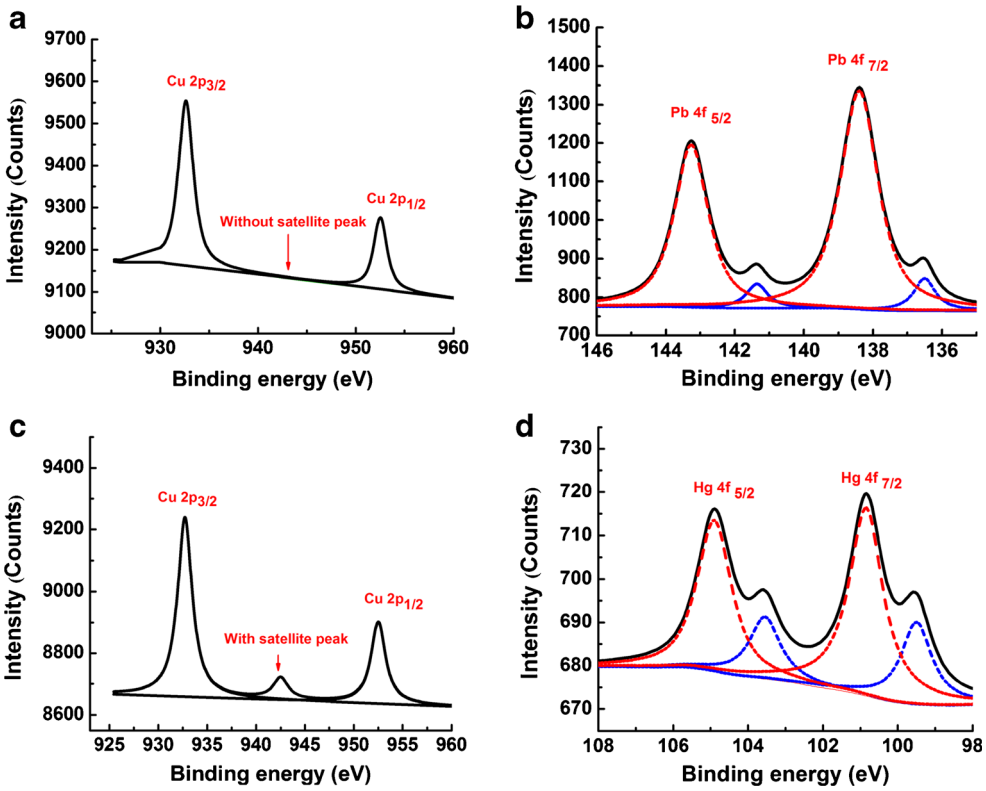

Fig. 2 XPS spectra of the elements (Cu, Pb, Hg) in the absence and presence of Pb^{2+}/Hg^{2+}. **a** Cu 2p curve of MT-CuNCs. **b** Pb 4f curve in MT-CuNCs-Pb^{2+} system. **c** Cu 2p curve in MT-CuNCs-Hg^{2+} system. **d** Hg4f curve in MTs-CuNCs-Hg system. The solutions of MT-CuNcs and MT-CuNCs-Pb^{2+}/Hg^{2+} were prepared respectively. XPS measurement were performed after vacuum drying at low temperature. $c_{Pb(II)} = 10$ μM, $c_{Hg(II)} = 2.0$ μM

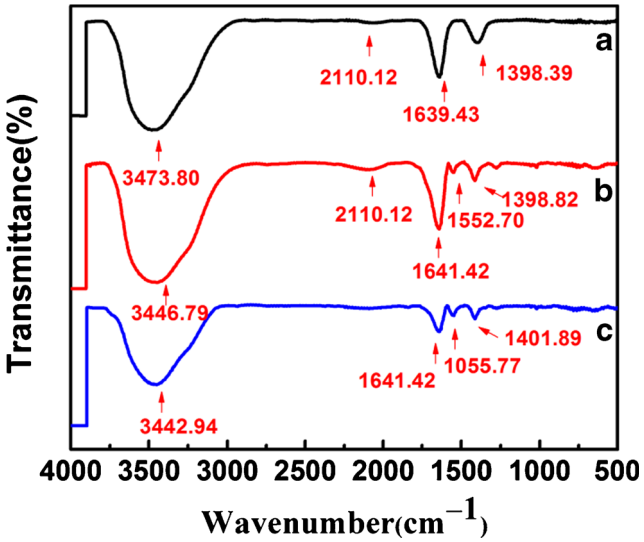

Fig. 3 Fourier transform infrared spectrum of MT-CuNCs in (**a**) the absence and presence of (**b**) Pb^{2+} or (**c**) Hg^{2+}. The solutions of the systems (MT-CuNCs, MT-CuNCs-Pb^{2+} and MT-CuNCs-Hg^{2+}) were prepared respectively. The solutions were dropped onto KBr flakes for determination. $c_{Pb(II)} = 10$ μM, $c_{Hg(II)} = 2.0$ μM

reaction with Pb^{2+}, the number of hydrogen bonds (at 3000–3600 cm^{-1}) in the MT-CuNCs system is increased, and the asymmetric stretching vibration of $^{+}N\text{-}H\cdots O^{-}$ (at 2110 cm^{-1}) is intensified [26], along with the production of the N-H stretching peak (amide II bonds, at 1552 cm^{-1}). Likewise, after the interaction between Hg^{2+} and MT-CuNCs, the transmittance values of the bands corresponding to C-N/C-C (amide III bonds, at 1398 cm^{-1}), C=O/N-H (amide I bonds, at 1641 cm^{-1}) and N-H/O-H decrease significantly, and bands corresponding to amide II bonds appear [27]. All these indicate that the interactions among Pb^{2+}/Hg^{2+}, Cu/Cu^{+} and MT change the coordination bonds in the MT-CuNCs.

Steady-state kinetic analysis The affinity of MT-CuNCs-Pb^{2+}/Hg^{2+} for H_2O_2 and TMB was investigated via steady-state kinetic analysis [28]. The results (Figs. S5 and S6) show that after the reaction between the MT-CuNCs and Pb^{2+}/Hg^{2+}, the process of catalyzing the TMB-H_2O_2 reaction follow the typical Michaelis-Menten model (a, b). Using the Lineweaver-Burk double-reciprocal method, it is found that there is a positive correlation between the reciprocal of the initial rate ($1/v$) and the reciprocal of the TMB concentration (1/[S]) (c, d) [29]. After linear fitting, the values of maximum reaction rate (v_{max}) and the Michaelis constant (K_m) were received. The affinities of MT-CuNCs-Pb^{2+}/Hg^{2+} ($K_m = 1.08/3.45$) for H_2O_2 is higher than that of HRP for H_2O_2 ($K_m = 3.70$), showing that only a small amount of H_2O_2 is enough to commence the catalytic oxidation reaction in the MT-CuNC-Pb^{2+}/Hg^{2+} systems (Table S1).

Detection of Pb^{2+} and Hg^{2+} In order to improve analysis performance, the reaction conditions were optimized (Figs. S7 - S12). Under the selected reaction conditions, the selectivity of this method for Pb^{2+} was investigated with a 10 μM Pb^{2+} solution as a reference. According to the experimental results (Fig. S12a), within a relative deviation of ±5%, species at 500 times (Zn^{2+} or Na^{+}), 250 times (Mg^{2+}, K^{+}, or Cd^{2+}), 100 times (Ca^{2+} or Mn^{2+}), 50 times (Al^{3+}), 25 times (Ag^{+} or Cu^{2+}), and 10 times (Hg^{2+} or Fe^{3+}) greater concentrations do not interfere with the determination of Pb^{2+}. Moreover, in the system for Hg^{2+} determination, the influence of several likely interfering components on the determination of Hg^{2+} was tested with a 2 μM Hg^{2+} solution as a reference. Within a relative deviation of ±5%, species at 500 times (K^{+} or Ca^{2+}), 250 times (Na^{+} or Cd^{2+}), 100 times (Mg^{2+}, Zn^{2+}, Mn^{2+} or Pb^{2+}), 50 times (Al^{3+}), 25 times (Ag^{+} or Cu^{2+}), and 10 times (Fe^{3+}) greater concentrations do not interfere with the determination of Hg^{2+} (Fig. S12b). In other words, this approach has great selectivity performance.

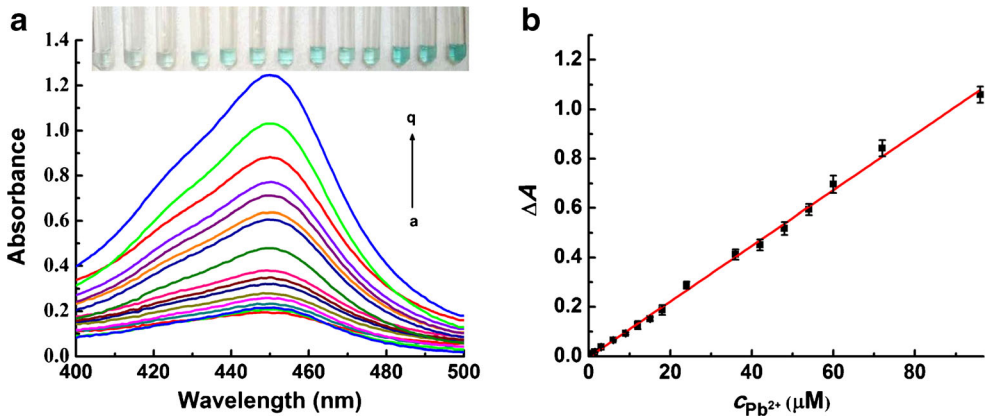

Fig. 4 **a** Absorption spectra (at 450 nm) of the TMB-H_2O_2-MT-CuNCs system in the absance and presence of different Pb^{2+} concentrations (from a to q: 0, 0.75, 1.5, 3, 6, 9, 12, 15, 18, 24, 36, 42, 48, 54, 60, 72, and 96 μM). Insert: the chromogenic photograph of different Pb^{2+} concentrations (from left to right: 0, 1.5, 6, 12, 18, 24, 36, 42, 48, 54, 60, 72, 96 μM). The photograph was obtained without performing acid termination, because blue is easier to distinguish than yellow. **b** Calibration plot of Pb^{2+} detection (concentration is consistent with that in the absorption spectra)

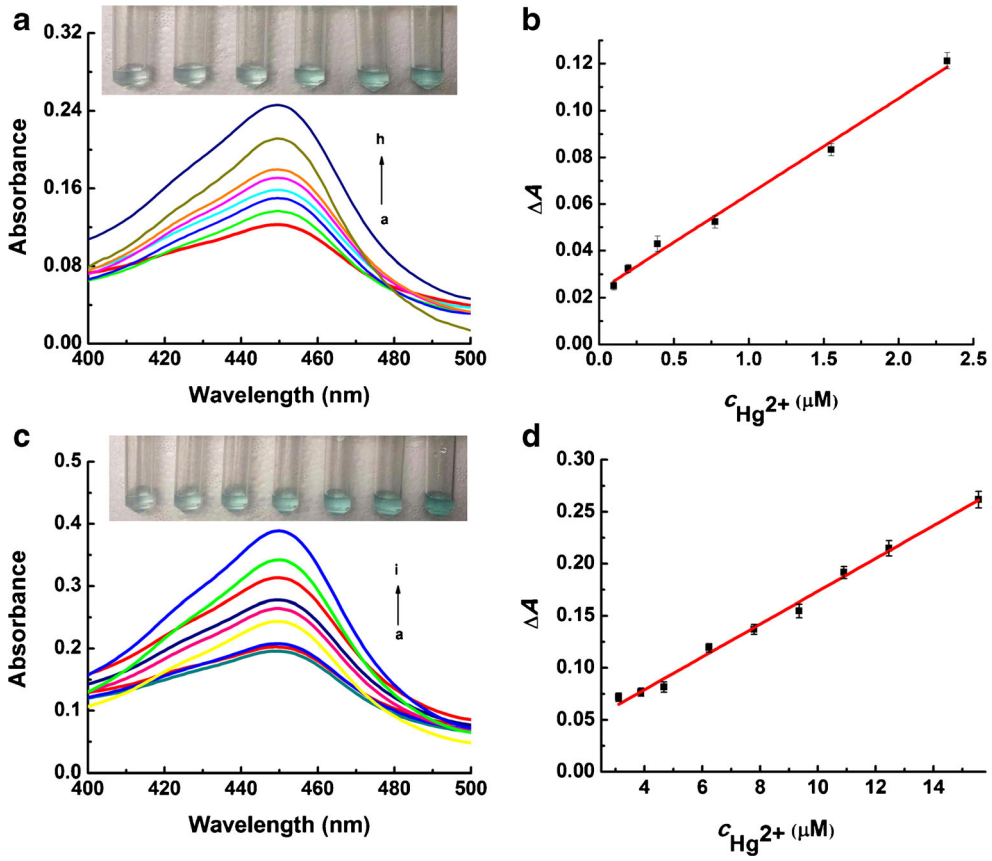

Fig. 5 Absorption spectra (at 450 nm) of the TMB-H_2O_2-MT-CuNCs system in the absance and presence of different Hg^{2+} concentrations. Insert: the chromogenic photograph of different Hg^{2+} concentrations. The photograph was obtained without performing acid termination. **a** (from a to h: 0, 0.097, 0.195, 0.39, 0.775, 1.55, and 2.325 μM). Insert: (from left to right: 0, 0.097, 0.39, 0.775, 1.55, and 2.325 μM). **c** (from a to i: 3.1, 3.875, 4.672, 6.23, 7.788, 9.345, 10.903, 12.46, and 15.56 μM). Insert: (from left to right: 3.1, 4.672, 7.788, 9.345, 10.903, 12.46, and 15.56 μM). **b, d** Calibration plot of Hg^{2+} detection (concentration is consistent with that in the absorption spectra)

The calibration plot for the determination of Pb^{2+} and Hg^{2+} were plotted under the optimized experimental conditions. Within the concentration range $c_{Pb(II)}$ of 707 nM-96 μM, a great linear relationship is observed (Fig. 4). The equation of linear regression was $\Delta A = 0.0113c_{Pb(II)}$ (μM)-0.034 with a correlation coefficient (r) of 0.9987. The detection limit (LOD) was calculated to be 142 nM based on the equation $LOD = 3S_b/k$. Precision experiments ($n = 11$) were carried out for three standard solutions with Pb^{2+} concentrations of 1.5, 60, and 96 μM. The relative standard deviations were 1.65%, 0.5% and 3.11%, respectively. These results show that this method for detecting Pb^{2+} has high accuracy. In the $c_{Hg(II)}$ ranges of 97 nM-2.325 μM and 3.10 μM–15.59 μM, the ΔA value and Hg^{2+} concentration are in a good linear relationship (Fig. 5). The regression equations were $\Delta A = 0.0413c_{Hg(II)}$ (μM) + 0.0231 (r = 0.9950) and $\Delta A = 0.0157c_{Hg(II)}$ (μM) + 0.0159 (r = 0.9961), respectively. LOD of this method was 43.8 nM. Three standard Hg^{2+} solutions

Table 1 Comparison of this approach with other methods for detecting Pb^{2+}/Hg^{2+}

Probe	Analyte	Method	Linear range	LOD	Reference
GSH-AuNCs	Pb^{2+}	Colorimetric	2–250 μM	2 μM	[13]
CdT4 Quantum dots (QDs)	Pb^{2+}	Fluorescence	2–100 μM	270 nM	[30]
Papain-AuNPs	Pb^{2+}	Colorimetric	Not available	200 nM	[31]
GSH-AuNPs	Pb^{2+}	Colorimetric	0.1–100 μM	100 nM	[32]
Protamine-AuNCs	Pb^{2+}	Fluorescence	80 nM-15 μM	24 nM	[23]
MT-CuNCs	Pb^{2+}	Colorimetric	707 nM-96 μM	142 nM	This Work
SiO_2/AgNPs	Hg^{2+}	Colorimetric	0–40 μM	5 μM	[33]
MoS_2 nanosheets	Hg^{2+}	Colorimetric	2–200 μM	500 nM	[15]
Papain-AuNPs	Hg^{2+}	Colorimetric	Not available	200 nM	[31]
Silica NPs	Hg^{2+}	Fluorescence	0–500 nM	20 nM	[34]
Cu@AuNPs	Hg^{2+}	Colorimetric	10–500 nM, 500–2500 nM	10 nM	[35]
MT-CuNCs	Hg^{2+}	Colorimetric	97 nM-2.325 μM, 3.10 μM–15.59 μM	43.8 nM	This Work

with concentrations of 0.775, 2.325, and 12.46 μM were each measured 11 times, and the relative standard deviations were 3.02%, 1.62%, and 2.32%, respectively. These demonstrate that the precision of this method for detecting Hg^{2+} is good. In comparison with other analytical methods for Pb^{2+}/Hg^{2+} determination, the data in the Table 1 show that the method for detecting Pb^{2+}/Hg^{2+} has a wide linear range and relatively good sensitivity.

Also, the method was employed to determine the ion concentrations in environmental water samples. After filtering twice with quantitative filter paper, all environmental water samples (collected from tap water, the pond water, Xiangjiang River,) were heated and boiled for 10 min. After cooling to room temperature, the solution was filtered through a 0.22 μm filter membrane for subsequent analysis. The recovery test of spiked samples were performed. The results (Tables S2,S3) demonstrate obviously that this method can be supplied for environmental water samples.

Conclusions

The relative catalase-like activity of MT-CuNCs is 2.8 times that of 1.5 mg·mL^{-1} CAT. Due to the generation of the Pb-Cu/Hg-Cu alloy, Pb^{2+}/Hg^{2+} induced the conversion of the catalase-like enzymatic activity of MT-CuNCs to peroxidase-like enzymatic activity. The latter catalyzed TMB-H_2O_2 oxidation according to a typical Michaelis-Menten model, and exhibited a higher affinity for H_2O_2 than HRP. Furthermore, a reliable colorimetry/spectrophotometry method for detecting Pb^{2+}/Hg^{2+} was established.. which had great selectivity, wide linear ranges and high sensitivity. The assay displays potential application for monitoring Pb^{2+}/Hg^{2+} concentration in environmental water sample.

Acknowledgments The authors gratefully acknowledge the support of the National Natural Science Foundation of China (No. 81473021).

Compliance with ethical standards The authors declare that they have no competing interests.

References

1. Zhang HL, Ma KX, Yang YJ, Shi CY, Chen GW, Liu DZ (2018) Molecular cloning, characterization, expression and enzyme activity of catalase from planarian Dugesia japonica in response to environmental pollutants. Ecotoxicol Environ Saf 165:88–95
2. Shi Y, Yang M, Liu L, Pang Y, Long Y, Zheng H (2018) GTP as a peroxidase-mimic to mediate enzymatic cascade reaction for alkaline phosphatase detection and alkaline phosphatase-linked immunoassay. Sensors Actuators B Chem 275:43–49
3. Zhang T, Cao C, Tang X, Cai Y, Yang C, Pan Y (2017) Enhanced peroxidase activity and tumour tissue visualization by cobalt-doped magnetoferritin nanoparticles. Nanotechnology 28:045704
4. Wei H, Wang E (2008) Fe_3O_4 magnetic nanoparticles as peroxidase mimetics and their applications in H_2O_2 and glucose detection. Anal Chem 80:2250–2254
5. Tao Y, Lin YH, Huang ZZ, Ren JS, Qu X (2013) Incorporating graphene oxide and gold nanoclusters: a synergistic catalyst with surprisingly high peroxidase-like activity over a broad pH range and its application for cancer cell detection. Adv Mater 25:2510–2510
6. Tao Y, Lin YH, Ren J, Qu X (2013) A dual fluorometric and colorimetric sensor for dopamine based on BSA-stabilized Au nanoclusters. Biosens Bioelectron 42:41–46
7. Liu Y, Ding D, Zhen YL, Guo R (2017) Amino acid-mediated 'turn-off/turn-on' nanozyme activity of gold nanoclusters for sensitive and selective detection of copper ions and histidine. Biosens Bioelectron 92:140–146
8. Santhosh M, Chinnadayyala SR, Kakoti A, Goswami P (2014) Selective and sensitive detection of free bilirubin in blood serum using human serum albumin stabilized gold nanoclusters as fluorometric and colorimetric probe. Biosens Bioelectron 59:370–376
9. Tao Y, Lin Y, Huang Z, Ren J, Qu X (2012) Poly(acrylic acid)-templated silver nanoclusters as a platform for dual fluorometric turn-on and colorimetric detection of mercury (II) ions. Talanta 88:290–294
10. Li CL, Liu KT, Lin YW, Chang HT (2011) Fluorescence detection of lead(II) ions through their induced catalytic activity of DNAzymes. Anal Chem 83:225–230
11. Li T, Dong SJ, Erkang W (2009) Label-free colorimetric detection of aqueous mercury ion (Hg^{2+}) using Hg^{2+}-modulated G-quadruplex-based DNAzymes. Anal Chem 81:2144–2149
12. Zhu R, Zhou Y, Wang XL, Zhang HJ, Huang XX, Zheng HZ (2013) Detection of Hg^{2+} based on the selective inhibition of peroxidase mimetic activity of BSA-Au clusters. Talanta 117:127–132
13. Liao H, Liu G, Liu Y, Li R, Fu W, Hu L (2017) Aggregation-induced accelerating peroxidase-like activity of gold nanoclusters and their applications for colorimetric Pb(2+) detection. Chem Commun (Camb) 53:10160–10163
14. Tseng CW, Chang HY, Chang JY, Huang CC (2012) Detection of mercury ions based on mercury-induced switching of enzyme-like activity of platinum/gold nanoparticles. Nanoscale 4:6823–6830
15. Lu Y, Yu J, Ye WC, Xin Y, Zhou PP, Zhang HX (2016) Spectrophotometric determination of mercury(II) ions based on their stimulation effect on the peroxidase-like activity of molybdenum disulfide nanosheets. Mikrochim Acta 183:2481–2489
16. Zhang HC, Ma KX, Yang YJ, Shi CY, Chen GW, Liu DZ (2018) Molecular cloning, characterization, expression and enzyme activity of catalase from planarian Dugesia japonica in response to environmental pollutants. Ecotoxicol Environ Saf 165:88–95
17. Liao H, Hu L, Zhang Y, Yu X, Liu Y, Li R (2018) A highly selective colorimetric sulfide assay based on the inhibition of the peroxidase-like activity of copper nanoclusters. Mikrochim Acta 185:143
18. Liu B, Huang Z, Liu J (2016) Boosting the oxidase mimicking activity of nanoceria by fluoride capping: rivaling protein enzymes and ultrasensitive F(−) detection. Nanoscale 8:13562–13567
19. Liu B, Liu J (2015) Accelerating peroxidase mimicking nanozymes using DNA. Nanoscale 7:13831–13835
20. Lien CW, Chen YC, Chang HT, Huang CC (2013) Logical regulation of the enzyme-like activity of gold nanoparticles by using heavy metal ions. Nanoscale 5:8227–8234
21. Bhamore JR, Jha S, Mungara AK, Singhal RK, Sonkeshariya D, Kailasa SK (2016) One-step green synthetic approach for the preparation of multicolor emitting copper nanoclusters and their applications in chemical species sensing and bioimaging. Biosens Bioelectron 80:243–248
22. Han A, Xiong L, Hao S, Yang Y, Li X, Fang G, Liu J, Pei Y, Wang S (2018) Highly bright self-assembled copper nanoclusters: a novel Photoluminescent probe for sensitive detection of histamine. Anal Chem 90:9060–9067

23. Huang YQ, Yang LN, Wang YS, Xue JH, Chen SH (2018) Protamine-stabilized gold nanoclusters as a fluorescent nanoprobe for lead(II) via Pb(II)-Au(I) interaction. Mikrochim Acta 185:483
24. Li JR, Xuan W, Li XP, Xiong CH, Wang XC (2010) Research progress in metallothionein. Food Sci 31:392–396
25. Huang YQ, Fu S, Wang YS, Xue JH, Xiao XL, Chen SH, Zhou B (2018) Protamine-gold nanoclusters as peroxidase mimics and the selective enhancement of their activity by mercury ions for highly sensitive colorimetric assay of Hg(II). Anal Bioanal Chem 410: 7385–7394
26. Vener MV, Odinokov AV, Wehmeyer C, Sebastiani D (2015) The structure and IR signatures of the arginine-glutamate salt bridge. Insights from the classical MD simulations. J Chem Phys 142:215106
27. Yan Z, Niu Q, Mou M, Wu Y, Liu X, Liao S (2017) A novel colorimetric method based on copper nanoclusters with intrinsic peroxidase-like for detecting xanthine in serum samples. J Nanopart Res 19:235
28. Wang GL, Dong YM, Jin LY, Wu XM, Li ZY (2015) Intrinsic enzyme mimicking activity of gold nanoclusters upon visible light triggering and its application for colorimetric trypsin detection. Biosens Bioelectron 64:523–529
29. Hu L, Yuan Y, Zhang L, Zhao S, Majeed J, Xu G (2013) Copper nanoclusters as peroxidase mimetics and their applications to H2O2 and glucose detection. Anal Chim Acta 762:83–86
30. Wu HM, Liang JG, Han HY (2008) A novel method for the determination of Pb^{2+} based on the quenching of the fluorescence of CdTe quantum dots. Microchim Acta 161:81–86
31. Guo YM, Wang Z, Qu WS, Shao HW, Jiang XY (2011) Colorimetric detection of mercury, lead and copper ions simultaneously using protein-functionalized gold nanoparticles. Biosens Bioelectron 26:4064–4069
32. Chai F, Wang C, Wang TT, Li L, Su ZM (2010) Colorimetric detection of Pb^{2+} using glutathione functionalized gold nanoparticles. ACS Appl Mater Interfaces 2:1466–1470
33. Rameshkumar P, Manivannan S, Ramaraj R (2013) Silver nanoparticles deposited on amine-functionalized silica spheres and their amalgamation-based spectral and colorimetric detection of Hg(II) ions. J Nanopart Res 15:1639–1647
34. Zhang YF, Yuan Q, Chen T, Zhang XB, Chen Y, Tan WH (2012) DNA-capped mesoporous silica nanoparticles as an ion-responsive release system to determine the presence of mercury in aqueous solutions. Anal Chem 84:1956–1962
35. Zhao Y, Qiang H, Chen ZB (2017) Colorimetric determination of Hg(II) based on a visually detectable signal amplification induced by a Cu@Au-Hg trimetallic amalgam with peroxidase-like activity. Microchim Acta 184:107–115